

# A PARALLEL EVOLUTIONARY MULTIPLE-TRY METROPOLIS MARKOV CHAIN MONTE CARLO ALGORITHM FOR SAMPLING SPATIAL PARTITIONS

Wendy K. Tam Cho<sup>1</sup>  
Yan Y. Liu<sup>2</sup>

## Abstract

We develop an Evolutionary Markov Chain Monte Carlo (EMCMC) algorithm for sampling spatial partitions that lie within a large and complex spatial state space. Our algorithm combines the advantages of evolutionary algorithms (EAs) as optimization heuristics for state space traversal and the theoretical convergence properties of Markov Chain Monte Carlo algorithms for sampling from unknown distributions. Local optimality information that is identified via a directed search by our optimization heuristic is used to adaptively update a Markov chain in a promising direction within the framework of a Multiple-Try Metropolis Markov Chain model that incorporates a generalized Metropolis-Hasting ratio. We further expand the reach of our EMCMC algorithm by harnessing the computational power afforded by massively parallel architecture through the integration of a parallel EA framework that guides Markov chains running in parallel.

*Keywords:* Markov Chain Monte Carlo; Evolutionary Algorithms; Spatial Partitioning

---

<sup>1</sup> Department of Political Science, Department of Statistics, Department of Mathematics, Department of Asian American Studies, the College of Law, and the National Center for Supercomputing Applications, University of Illinois at Urbana-Champaign. [wendycho@illinois.edu](mailto:wendycho@illinois.edu)

<sup>2</sup> Research Scientist, Computational Urban Sciences Group, Computational Science and Engineering Division, Oak Ridge National Laboratory. [yanliu@ornl.gov](mailto:yanliu@ornl.gov)

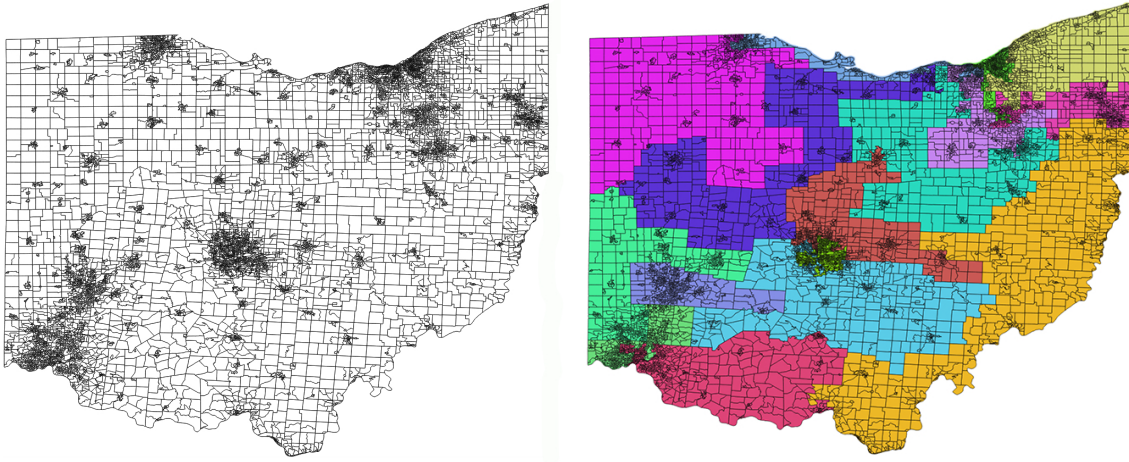


Figure 1: Spatial Geographic Units that Encompass the State of Ohio and a Particular Spatial Partition of those Units into 16 Disjoint Contiguous Zones

## 1 Introduction

Markov Chain Monte Carlo (MCMC) methods originated in statistical physics (Metropolis et al., 1953) and have migrated to applications in many disciplines. A particular use of MCMC that has wide application is for sampling from complex and unknown distributions. While the theory of MCMC methods ensures sampling from unknown distributions, it is not always straightforward to devise these methods for a particular application, and the theoretical result, moreover, is asymptotic. Indeed, if the application problem is large and the state space is difficult to traverse, the amount of time required before the theoretical convergence of a Markov chain is realized may be prohibitively long. Hence, while MCMC methods are theoretically attractive, successful implementation for complex applications can be quite challenging.

Consider the spatial partitioning application illustrated in Figure 1. The goal is to characterize the set of all possible feasible partitions of size  $k$ , where feasible is defined as a partition that satisfies a specific set of constraints (e.g., contiguity). The plot on the left displays a fixed set of geographic units that collectively encompasses the entire state of Ohio. The plot on the right shows one particular mutually exclusive and exhaustive partition of these geographic units into  $k = 16$  disjoint contiguous sets. One can visually see that, given the large number of base geographic units, there is an enormous number of distinct partitions into 16 disjoint contiguous sets. Indeed, this number is sufficiently large that it is computationally infeasible to enumerate the set of all partitions within current computing capabilities. Since an exhaustive search is not possible, an alternative route is to produce a representative sample of the universal set, which would also allow us to derive insights into the underlying population of feasible partitions. MCMC methods provide a possible route for sampling from this unknown population distribution. However, how to specify an MCMC model that produces a sample of feasible spatial partitions is not obvious.

For many applications, a common MCMC strategy is to define a Markov transition function that amounts to a small or local random change in the current state. Small or local changes are

attractive for two reasons. First, they are conceptually and operationally simple—these moves are easy to define and relatively simple to implement. Second, the Metropolis-Hastings ratio (Metropolis et al., 1953; Hastings, 1970) needs to regularly lead to accepted transition proposals. Since a small change likely results in a large Metropolis-Hastings ratio, the movement of the Markov chain is then fairly fluid. At the same time, because these are small movements in a very large state space, the resulting Markov chain converges slowly and is, moreover, likely to become trapped in localized regions. Hence, for large or complex applications, though this type of chain may be simple to specify, it is not likely to converge rapidly enough to be practically useful. In this case, performance is compromised for conceptual ease.

For the spatial partitioning application, given a feasible state, a small or local random change might be to choose a geographic unit on a zone border and reassign it to an adjacent zone. This type of movement is conceptually and operationally simple, both to understand and to implement. One can see, however, that when there are a large number of geographic units, relying solely on this type of movement to traverse the underlying population of feasible partitions would be inefficient, and likely prohibitively so.

To improve performance and hasten convergence, one approach is to define larger steps for the Markov chain. Two particular benefits accrue from pursuing this strategy. First, larger moves may enable a chain to escape from local optimal states. Second, if well-designed, these larger moves can more efficiently and effectively traverse a large state space, leading to faster convergence of the chain. However, how to conceive intelligent and large movements that effectively transition from one feasible partition to another feasible partition is not easily discernible. Simply “large” movements are likely to result in small Metropolis-Hastings ratios, which lead to rejected proposals, and thus to a non-fluid and ineffective Markov chain.

Plainly, a central goal for an effective MCMC algorithm is to devise a chain that is able to traverse the state space in both an effective and efficient manner. Notably, effective and efficient solution space traversal is precisely the same objective that animates the research on optimization heuristics. Here, we examine how insights that have been gleaned from the optimization heuristics literature might be adapted to improve the performance of MCMC algorithms for the spatial partitioning problem. The main task in marrying these two literatures is to fit the mechanics of the optimization search within the MCMC theoretical framework that enables sampling.

## 2 Intelligent State Space Traversal

### 2.1 Gibbs Sampler

Intelligent and randomized state space traversal are fundamental to performance, whether for an optimization heuristic or for an MCMC algorithm. One way in which the moves can be both random and purposeful rather than simply random, is to follow the local dynamics of the target distribution. A Gibbs sampler follows the local dynamics of the target distribution by composing a sequence of conditional distributions along a set of sampling directions. In practice, while Gibbs samplers are ensured theoretical convergence, they may converge quite slowly, because it is often not clear how to intelligently sample from the full conditional distributions.

In the Gibbs sampler, we wish to sample from  $f(\mathbf{x})$  where  $\mathbf{x}$  can be broken down into components,  $\mathbf{x} = (x_1, x_2, \dots, x_n)$ . One iteration of a systematic scan Gibbs sampler can be described as follows. Begin at some state,  $\mathbf{x}^{(0)}$ . At iteration  $i$ ,

1. Sample  $x_1^{(i+1)}$  from the conditional distribution  $f(x_1 | x_2^{(i)}, x_3^{(i)}, \dots, x_n^{(i)})$ .
2. Sample  $x_2^{(i+1)}$  from the conditional distribution  $f(x_2 | x_1^{(i+1)}, x_3^{(i)}, \dots, x_n^{(i)})$ .
- $\vdots$
- n. Sample  $x_n^{(i+1)}$  is sampled from  $f(x_n | x_1^{(i+1)}, x_2^{(i+1)}, \dots, x_{n-1}^{(i+1)})$

The sequence of realizations,  $\{\mathbf{x}^{(t)} = (x_1^{(t)}, x_2^{(t)}, \dots, x_n^{(t)})\}$ , forms a Markov chain with stationary distribution,  $f(\mathbf{x})$ .

Two challenges must be overcome for the Gibbs sampler to be successful. First is the issue of *conjugacy* or the ability to sample from the conditional distributions (Carlin and Gelfand, 1991). Second is how to overcome the difficulty in constructing univariate sampling directions in such a way that ensures rapid movement around the support of  $f(\mathbf{x})$  when simple random movement is insufficient. In other words, while it is possible to devise a Gibbs sampler that follows the local dynamics of the target distribution, how precisely one intelligently, and thus effectively, devises this movement is non-obvious and, further, application dependent.

The conjugacy issue can be addressed with the Griddy-Gibbs sampler (Ritter and Tanner, 1992) where rather than sampling from the full conditional distributions, one may form a simple approximation of the inverse CDF on a grid of points. However, even with a successful implementation of the Griddy-Gibbs sampler that addresses the difficulties of sampling from the full conditional distributions, the challenge of devising intelligent movements in purposeful directions remains.

## 2.2 Adaptive Direction Sampling

Adaptive Direction Sampling (ADS) is a general technique that fits within the framework of the Gibbs sampler and aims to sample in a particular search direction. It was introduced as an automated way of overcoming the slow convergence in the Gibbs sampler by providing a way to guide sampling from the conditional distributions (Gilks, Roberts and George, 1994; Roberts and Gilks, 1994). The ADS algorithm also introduces a way in which the interaction of multiple Markov chains can be specified to improve the performance of MCMC by proposing that the sampling direction be updated with information from a different Markov chain state.

ADS can be adapted in various ways. The general form of ADS is

$$\mathbf{x}_c^{(t+1)} = \mathbf{x}_c^{(t)} + r(\mathbf{v}^{(t)} + u^{(t)}\mathbf{x}_c^{(t)}), \quad (1)$$

where  $\mathbf{v}^{(t)}$ , an  $n$ -vector, and  $u^{(t)}$ , a scalar, are any functions of the current set,  $\mathbf{S}(t)$ , excluding  $\mathbf{x}_c^{(t)}$ , the current state, all at time or state  $t$ . If  $\mathbf{v}^{(t)}$  is the difference between two points in the current set, parallel ADS emerges. If  $\mathbf{v}^{(t)}$  is a random coordinate direction with  $u^{(t)} = 0$ , we have the Gibbs sampler. The hit-and-run algorithm emerges when  $\mathbf{v}^{(t)}$  is a random direction and  $u^{(t)} = 0$  (Bélisle, Romeijn and Smith, 1993).

Although adapting the direction of the sampling with information from another state can clearly be helpful, the core problem with intelligent state space traversal remains. Indeed, studies of the ADS algorithm indicate that it is not particularly effective for improving sampling efficiency generally if the direction generated by ADS remains rather arbitrary. Instead, moving in the direction of the other chains improves the state space traversal only when such movement coincides with transitions that are intelligent and purposeful.

### 2.3 Adaptive Direction Sampling Guided by Evolutionary Algorithm Operators

Rather than relying on an arbitrary direction, Liang and Wong (2001) guide the directional sampling of ADS with their *snooker crossover*, a recombination operator from an evolutionary algorithm (EA) that they modify to fit within the MCMC framework. That is, they utilize an optimization heuristic to define the sampling direction in ADS. In the snooker algorithm, a set of possible states,  $\mathbf{S}$ , is retained. In the language of evolutionary algorithms, these possible states comprise the population. From the set,  $\mathbf{S}$ , two states are chosen randomly, one as the current state,  $\mathbf{x}_c$ , and one as the anchor state,  $\mathbf{x}_a$ . The direction of movement is then chosen along a line that connects the current state and the anchor state. From equation (1), the snooker algorithm arises when  $u^{(t)} = -1$  and  $\mathbf{v}^{(t)} = \mathbf{x}_a^{(t)}$ , where  $\mathbf{x}_a^{(t)}$  is a randomly chosen state from  $\mathbf{S}(t)$ , excluding  $\mathbf{x}_c^{(t)}$ . To prevent the new states from being too concentrated around the anchor state, one can sample from an adjusted full conditional distribution. The intuition is that after a burn-in period, the set of states is likely to be in high density regions, and high density states are helpful for identifying sampling directions for a Gibbs sampler.

While the snooker algorithm is a recombination evolutionary algorithm operator that can be adapted to fit within the mathematical framework of MCMC, the effectiveness and efficiency of the algorithm for recovering samples for any particular application is still dependent on how its operators traverse that *particular* state space. In the optimization literature, it is clear that while EAs have been successful for many applications, significant effort must still be expended to adapt the heuristic to the particular solution landscape. To be sure, EAs are not panaceas. Rather, they comprise a general technique whose success is dependent on successful adaptation of the evolutionary framework to a specific application.

All the same time, combining optimization heuristics within an MCMC framework is a promising strategy for difficult problems, and one that has already been successfully implemented for a number of interesting problems, including Bayesian mixture models,  $C_p$  model sampling, and change point problems (Liang and Wong, 2000, 2001; Laskey and Myers, 2003). The main hindrance is that the approach is general, and successful implementation of both the optimization as well as the MCMC components, especially for complex applications, must be tuned to the idiosyncrasies of the application state space.

### 2.4 The Multiple-Try Method

Liu, Liang and Wong (2000) generalize how Markov chain movement can be adapted with optimization heuristics in their Multiple-Try Method (MTM). They propose a way to incorporate optimization steps into an MCMC sampler with a multiple-try Metropolis-like transition rule that

enables a more thorough exploration of the neighboring region that is defined by a transition proposal,  $T(\mathbf{x}, \mathbf{y})$ . The method is general and Liu, Liang and Wong (2000) demonstrate how MTM can be combined with different MCMC variants (in particular, ADS, Griddy-Gibbs samplers, and the Hit-and-Run algorithm) to produce more effective samplers.

In the MTM framework, suppose that the current state is  $\mathbf{x}$ . The optimization heuristic proposes some set of  $m$  proposal moves,  $\mathbf{Y} = \{\mathbf{y}_1, \dots, \mathbf{y}_m\}$ . In this way, the optimization heuristic provides a method for directional sampling without the shortcoming of previous approaches that relied primarily on a random direction. Importantly, since an optimization move may not be a proper Markov transition, it cannot simply be accepted as the next state in a Markov chain. Instead, from the set of proposal states created by the optimization heuristic, one proposal state,  $\mathbf{y} \in \mathbf{Y}$ , is selected probabilistically, and this selected proposal is then accepted or rejected according to a generalized Metropolis-Hastings ratio that has the form,

$$r_g = \min \left\{ 1, \frac{\xi(\mathbf{y}_1, \mathbf{x}) + \dots + \xi(\mathbf{y}_m, \mathbf{x})}{\xi(\mathbf{x}_1^*, \mathbf{y}) + \dots + \xi(\mathbf{x}_m^*, \mathbf{y})} \right\}, \quad (2)$$

where  $\xi(\mathbf{y}, \mathbf{x})$  is the probability of choosing proposal  $\mathbf{y}$  from the set  $\mathbf{Y}$ , and  $\{\mathbf{x}_i^*\}, i = 1, \dots, m$ , comprise a set of proposal moves from the same optimization heuristic that now begins at state  $\mathbf{y}$  and moves in the direction of state  $\mathbf{x}$ .

Liu, Liang and Wong (2000) develop and demonstrate these ideas with a Conjugate-Gradient Monte Carlo where the search direction proceeds along a vector whose direction is based on the conjugate gradient. Once the direction is chosen, randomness is injected via the magnitude of this vector. Searching along a gradient is one optimization technique, but plainly not the only option. This tactic is effective for certain types of state spaces, but not ideal for other types, and certainly not for all types. Indeed, optimization heuristics come in many different genres, and within these genres, with many different specifications and implementations. However, the MTM framework is general such that *any* optimization technique can be employed to create a set of proposal moves that are then accepted or rejected according to the generalized Metropolis-Hastings ratio.

The evolution of these algorithms highlights a theme encountered repeatedly both in statistical modeling and in the design of optimization heuristics. Namely, there is not one fixed solution that is ideal for every application. There are only general guiding principles for utilizing particular modeling frameworks. Incontrovertibly, devising Markov chains must be done with the peculiarities of the application in mind. As well, the success of optimization heuristics increases in likelihood when they are designed to adapt to application idiosyncrasies. In every case, circumspection is necessary in the selection of a meaningful and effective search direction for either the Markov chain transitions or the optimization heuristic steps.

### 3 An Evolutionary Algorithm for Spatial Optimization

While traversal of some state spaces may seem to fit into standard frameworks, other state spaces are more unusual. Constrained spatial state spaces produce particularly thorny applications since it is difficult to envision how one might transform multi-dimensional spatial characteristics into uni-dimensional searches. Indeed, spatial constraints pose particular problems for both spatial optimization as well as sampling techniques because spatial requirements can impose significant



## Constraints

$$\sum_{j | (i,j) \in A} y_{ijk} - \sum_{j | (j,i) \in A} y_{jik} = n_k h_{ik} - x_{ik} \quad \forall k \in K, \forall i \in I \quad (3)$$

$$\sum_{j | (j,i) \in A} y_{jik} \leq (n_k - 1)x_{ik} \quad \forall k \in K, \forall i \in I \quad (4)$$

$$\sum_{k \in K} x_{ik} = 1 \quad \forall i \in I \quad (5)$$

$$\sum_{i \in I} h_{ik} = 1 \quad \forall k \in K \quad (6)$$

$$a\mathbf{x} \leq b \quad (7)$$

$$x_{ik}, h_{ik} \in \{0, 1\} \quad \forall k \in K, \forall i \in I \quad (8)$$

$$y_{ijk} \geq 0 \quad \forall k \in K, \forall (i, j) \in A \quad (9)$$

The above formulation is revised from Shirabe (2009), who defines the contiguity for each partition as a network flow from all of the spatial units in each zone to their zone hub that receives the flow. The objective function,  $obj()$ , is a weighted sum of spatial and non-spatial objectives. Constraint (3) requires that the difference of flow into a unit  $i$  and out of  $i$  must be  $(n_k - 1)$ . This means that if unit  $i$  is the hub of zone  $k$ , the flow traverses each unit in the zone exactly once. Otherwise, this constraint has no effect. Constraint (4) ensures that no unit is visited twice. Constraint (5) guarantees that each unit is a member of one and only one zone. Constraint (6) guarantees that each zone has only one hub. These four constraints together ensure that all of the units are partitioned into exactly  $k$  contiguous zones. Constraint (7) denotes all other non-spatial constraints. While unit assignment is discrete (Constraint (8)), the flow is formulated as a continuous variable (Constraint (9)). We can also see that this problem is computationally intractable since Constraints (3) and (4) generate a number of inequalities that increases exponentially with the number of units.

One example of a constraint is the requirement for weight balancing across zones. Here, each spatial unit,  $u_j, j = 1, \dots, n$ , is associated with a weight,  $u_j^{(w)}$ . Each zone,  $i = 1, \dots, k$ , is an aggregation of some number of these units, and the weight for zone  $i$  is  $w_i = \sum_{u_j \in \text{zone } i} u_j^{(w)}$ . The aggregated weight for any one zone is required to be within a small specified range,  $\varepsilon$ , of all other zones,

$$\frac{\max_{i=1}^k w_i - \min_{i=1}^k w_i}{\sum_{i=1}^k w_i} < \varepsilon. \quad (10)$$

There are many other constraints that may be imposed on the solutions. One example is a mathematically defined shape requirements that may, for instance, constrain the size of the isoperimeter quotient or the ratio of the area of a zone to the area of a circle with the same perimeter. Another example of a spatial constraint is a requirement that certain spatial units must be contained in the same zone. While there are a large number of possibilities for spatial constraints, they all have the effect that they limit the global state space to a smaller feasible state space where feasibility is defined as states that satisfy these specific spatial and non-spatial constraints.



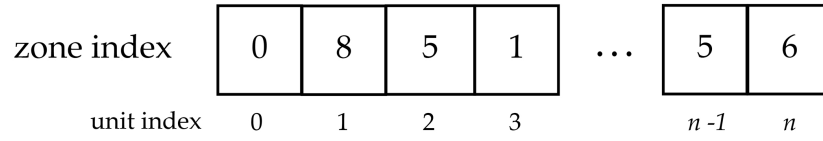


Figure 2: Chromosome encoding for spatial partitioning application

To formulate an EA for this spatial partitioning problem, we may encode the chromosome (shown in Figure 2) as an integer array with  $n$  alleles,  $\beta_1, \beta_2, \dots, \beta_n$ . Each allele,  $\beta_i$ , takes on one value from the set,  $[1, k]$ . We introduce a virtual unit 0 and its associated zone 0 to indicate the region border outside and surrounding the units being partitioned. Every spatial unit is assigned to exactly one zone.

This formulation is similar to the Real-Encoded Evolutionary Monte Carlo (Liang and Wong, 2001) except that  $\beta_i \in [0, k] \in \mathbb{Z}$  instead of  $\beta_i \in \mathbb{R}$ . While this may seem like a reduction in the solution space, note that in our application, the state space becomes much more complex since the spatial constraints *significantly* restrict which encodings are valid or feasible solutions and render most of the combinatorial encodings as infeasible because they violate the spatial constraints. In turn, the restrictions on which encodings are valid makes the solution space traversal especially difficult since randomly choosing alleles to alter is then very likely to result in a solution that violates the constraints. Movement in the solution space thus must be carefully considered and spatially aware to avoid wasted computational effort.

### 3.1.1 Spatial Mutation Operator

For this spatial partitioning optimization problem, Liu and Cho (2020) formulated two EA spatial operators. The first is an ejection chain-based mutation operator, ECMUT, which selects a chromosome at random and mutates a small number of its “mutable” alleles where an allele is defined as mutable if the change in the allele does not result in an infeasible solution. When a small number of alleles are mutated, at least one of the alleles is on a zone border. This process may be described as follows.

1. Randomly choose one chromosome,  $\mathbf{x}_i$  from the current population,  $\mathbf{S}$ .
2. Add a random vector subject to constraints,  $\mathbf{e}$ , to create a new chromosome  $\mathbf{y}_i = \mathbf{x}_i + \mathbf{e}$ , where  $\mathbf{e}$  is chosen so that  $\mathbf{y}_i$  is a feasible solution.

### 3.1.2 Spatial Path-Relinking Crossover Operator

The second EA operator is spatial path-relinking crossover operator (PRCRX) that adapts the general non-spatial path relinking method to the spatial context. It does so by providing an ordered way to explore and perform recombination in the neighborhood space defined by two chromosomes (Glover, 1994; Glover, Laguna and Marti, 2000) that respects spatial constraints. Details of their operators are provided in Liu and Cho (2020). Here, we provide just a general description.

In particular, their spatial path-relinking crossover can be described as follows. At step  $i$ ,

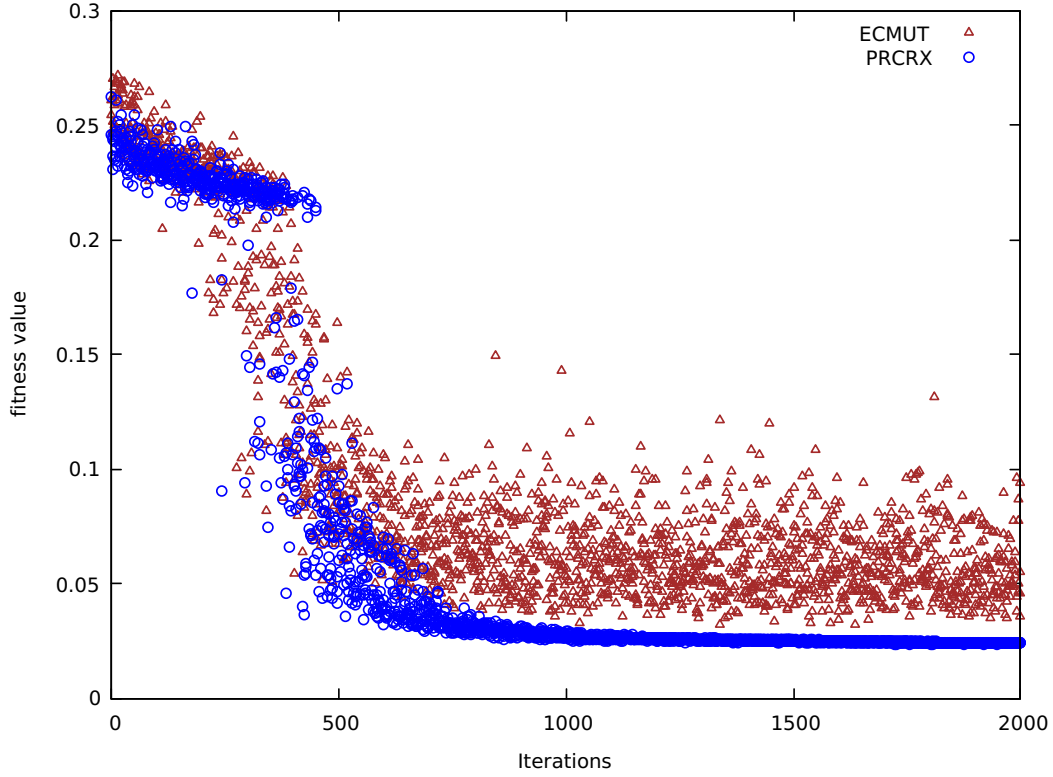


Figure 3: Performance of the Spatial Path Relinking Crossover Operator (PRCRX)

1. randomly choose two chromosomes, a source solution,  $\mathbf{x}_s$ , and a target solution,  $\mathbf{x}_t$ ,  $s \neq t$ , from the population  $\mathbf{S}^{(i)}$ .
2. The relinking process is comprised of a “walk” in the spatial neighborhood space between the two solutions. Each step in the path converts a random allele from its value in  $\mathbf{x}_s$  to its value in  $\mathbf{x}_t$ . It is possible that some of set of these steps will lead to infeasible solutions, though spatial contiguity is always maintained.
3. If feasible solutions are found on the path, randomly pick one,  $\mathbf{y}$ , to replace chromosome  $\mathbf{x}_s$  with some probability, yielding a new population,  $\mathbf{S}^{(i+1)}$ .

The ECMUT spatial mutation and PRCRX spatial crossover operators have been shown to be effective and efficient for a large spatial partitioning optimization application.

Figure 3 shows the performance of these EA operators in an optimization context. We can see from the figure that while ECMUT is also effective in identifying solutions with increasingly optimal values, the spatial path relinking operator provides significant additional improvement in the search process. In particular, PRCRX was able to reach lower fitness values more quickly and more deliberately than the ECMUT operator alone, which exhibited improved, but more variable, behavior.

In Liu and Cho (2020)’s empirical evaluation, they compared the performance of their EA operators with the performance of four previously proposed spatial optimizers and provided com-

elling evidence that for the spatial partitioning optimization problem, the ECMUT and PRCRX operators are more effective in guiding movement in promising search directions and thus identifying better solutions. Indeed, the idea of path relinking was originally developed to provide guided intelligence for seeking integer solutions along the path between two relaxed real-number solutions.

## 4 Evolutionary Spatial Sampling

Spatial optimization and spatial sampling share a common component, the need for effective and efficient traversal of a spatial state space. While operators that have been designed for spatial optimization cannot be used directly for sampling from spatial state spaces, they can be adapted to an MCMC framework either through a Metropolis-Hastings framework, for instance, or by providing a *proposal set* for directional sampling according to the structure of the Multiple-Try Metropolis MCMC model. We now discuss how this adaptation might proceed for these particular EA operators in the spatial partitioning problem.

### 4.1 ECMUT Mutation

ECMUT is a fairly small and local movement, simply exchanging some small number,  $p$ , of mutable units. The adaptation of the ECMUT mutation operator to define the transition of a Markov chain for a standard Metropolis-Hastings MCMC is theoretically straightforward. In particular, an ECMUT proposal is accepted with probability,  $\min(1, r)$ , defined by the Metropolis-Hastings rule, where

$$r = \frac{\pi(\mathbf{y}) T(\mathbf{y}, \mathbf{x})}{\pi(\mathbf{x}) T(\mathbf{x}, \mathbf{y})} = \exp\{-[H(\mathbf{y}) - H(\mathbf{x})]\} \frac{T(\mathbf{y}, \mathbf{x})}{T(\mathbf{x}, \mathbf{y})}, \quad (11)$$

and  $T(\mathbf{x}, \mathbf{y})$  is a proposal transition function. When the transition function,  $T(\cdot)$ , is symmetric (as it is for non-spatial state spaces, where every allele is subject to possible mutation and may be mutated to any other allele), only the fitness values are needed to compute the Metropolis-Hastings ratio.

For our application, the transition function is not symmetric because we constrain ECMUT movement to feasible alleles, at least one of which is located on a zone border. Hence, for the spatial partitioning problem, we calculate the MH ratio as

$$r_{MUT} = \frac{M_x}{M_y} \exp\{-[H(\mathbf{y}) - H(\mathbf{x})]\}, \quad (12)$$

where  $M_x$  is the number of mutable units that may be chosen for the mutation step that originates from solution  $\mathbf{x}$  and that results in another feasible solution. Similarly,  $M_y$  is the number of mutable units that may be chosen for the mutation step that originates from solution  $\mathbf{y}$  and that results in another feasible solution.  $H(\cdot)$  is the fitness function value for a particular solution.

To distinguish the use of the operator for differing numbers of mutated units, we call the operator ECMUT- $p$ , where  $p$  is the number of units that are mutated. Variations of ECMUT-1 as an MCMC transition proposal for spatial partitioning have been discussed by others (Bangia et al., 2017; Mattingly and Vaughn, 2014). For ECMUT-1,  $M_x$  and  $M_y$  are fairly straightforward to

compute because they can be enumerated with modest computational effort even for large spatial partitioning problems (Liu, Cho and Wang, 2016).

In particular, to compute  $M_s$ , where  $s$  is some solution, we can assess whether each boundary unit for each zone is mutable, which means that it can be reassigned to a neighboring zone without disconnecting its current zone and would result in a feasible solution after mutation. Notice that, for a planar graph, where the edges indicate unit connectivity, the computing cost for  $M_s$  depends on the number of neighbors that must be checked for contiguity for each unit on a zone boundary and the total number of zone boundary units. Because of the sparsity of a planar graph, the average cost of checking the direct neighbors of a zone boundary unit for mutability is  $O(1)$ . In addition, following the Euler characteristic, for any convex polyhedron surface,  $V - E + F = 2$ , where  $V$  is the number of vertices,  $E$  is the number of edges, and  $F$  is the number of faces. In our application,  $V = n$ , the number of units,  $E$  is the number of edges or adjacency links, and  $F$  is the number of faces in our resulting finite and connected planar graph. We know that  $E \leq 3n - 6$  when  $n \geq 3$  since any face is bounded by at least three edges, and each edge touches two faces. Therefore, for any unit, the average number of direct neighbors is less than three.

The relationship between  $b$ , the number of boundary units for all  $k$  zones, and  $n$  can be modeled as the total length of the zone perimeters and the sum of the zone areas. We can make an analogy to cutting a pizza into  $k$  pieces where the shape of each piece is inconsequential as long as the  $k$  pieces collectively encompass the whole pizza. Here, each pizza piece is akin to a zone. The upper bound of  $b$  is  $n$ , regardless of the value of  $k$ . For example, consider an  $n = q \times k$  grid, when each row of  $q$  cells is a zone in a  $k$ -partition solution. The lower bound of  $b$  is  $k$ . This would occur in the scenario where one zone has  $(n - k + 1)$  contiguous units while the  $(k - 1)$  remaining zones contain one unit from the rest of the  $(k - 1)$  units. Hence, we know that  $\frac{k}{n} \leq \frac{b}{n} \leq 1$ . An important observation is that, when  $k$  is fixed, the rate of decrease for the ratio,  $\frac{b}{n}$ , is faster than the rate of increase for  $n$ . That is, while the area increases linearly with  $n$ , the perimeter increases in proportion to  $\sqrt{n}$ . The manifestation in our problem is that, as the problem size increases, the cost of computing  $M_s$  rises much slower than the linear increase of  $n$ .

While ECMUT-1 provides a proper Markov transition with a computationally feasible MH ratio, we have already discussed the issues associated with the ECMUT-1 transition. First, while this type of transition in a Metropolis-Hastings MCMC is simple conceptually and operationally, and results in a fluid Markov chain, the performance of such an operationalization is inefficient and possibly insufficient if the state space is particularly large or complex. Unless the performance can be greatly improved, perhaps via massive computational resources, this type of transition proposal will be inadequate for large scale applications. Second, even for a relatively small spatial partitioning application, because the spatial constraints render large numbers of the combinatorial encodings as infeasible, this Markov chain is likely to become trapped in localized regions that are disconnected from other feasible solutions, resulting in a reducible chain that is incapable of sampling from the global state space.

An ECMUT- $p$  operator, where  $p > 1$ , produces larger transitions, which contributes to searching efficiency and reduces (though do not solve) the issues associated with disconnected state space regions since invalid encodings can be traversed between the first and the  $p$ th single unit step. If we are able to enumerate the set of possible transitions of size  $p$  from a solution  $\mathbf{x}$ , we can compute the MH ratio (12) directly. The tradeoff is, as  $p$  increases, this combinatorial calculation

becomes increasingly computationally expensive, requiring innovations in algorithmic sophistication.<sup>1</sup>

## 4.2 Crossover and Recombination

EA crossover operators have been successfully integrated into an MCMC framework. For example, Liang and Wong (2000) adapt a binary-encoded EA, where the alleles,  $\beta_i \in \{0, 1\}$ , produce a chromosome that is a binary vector. Their crossover operators include a 1-point, 2-point, and uniform crossover. They choose the first parent chromosome,  $x_i$  from the population,  $\mathbf{x}$ , using a roulette wheel. The second parent,  $x_j$ , is chosen randomly from the remaining chromosomes. From the two parent chromosomes, two offspring chromosomes,  $y_i$  and  $y_j$ , are generated. Without loss of generality, assume  $H(x_i) \geq H(x_j)$  and  $H(y_i) \geq H(y_j)$ . A new population,  $\mathbf{y} = \{x_1, \dots, y_i, \dots, y_j, \dots, x_n\}$ , is proposed and is accepted with probability,  $\min(1, r_c)$ , where

$$r_c = \frac{\pi(\mathbf{y}) T(\mathbf{y}, \mathbf{x})}{\pi(\mathbf{x}) T(\mathbf{x}, \mathbf{y})} = \exp\{-[H(y_i) - H(x_i)]/t_i - [H(y_j) - H(x_j)]/t_j\} \frac{T(\mathbf{y}, \mathbf{x})}{T(\mathbf{x}, \mathbf{y})} \quad (13)$$

is the Metropolis-Hastings ratio, and  $T(\mathbf{x}, \mathbf{y}) = P((x_i, x_j) | \mathbf{x}) P((y_i, y_j) | (x_i, x_j))$ . Within the transition probability,  $P((x_i, x_j) | \mathbf{x})$ , the probability of selecting  $(x_i, x_j)$  from the population  $\mathbf{x}$ , is

$$P((x_i, x_j) | \mathbf{x}) = \frac{1}{(n-1)Z(\mathbf{x})} [\exp[-H(x_i)/t] + \exp\{-H(x_j)/t\}], \quad (14)$$

where  $Z(\mathbf{x}) = \sum_{i=1}^n \exp\{-H(x_i)/t\}$ . Since this crossover operator is symmetric, the ratio of transition probabilities reduces to 1, and so only the selection probabilities, which are either chosen randomly or based on fitness values, are needed to determine the acceptance probability.

Real-encoded EAs can be more intimidating than binary-encoded EAs in the sense that the non-spatial real-encoded model,  $x = \{\beta_1, \beta_2, \dots, \beta_k\}$ , with  $\beta_i \in \mathbb{R}$ , encompasses a much larger solution space to traverse. However, when moving to the non-spatial real-encoded values no additional complications are introduced in the adaptation for symmetric transition probabilities. This occurs for simple crossover operators like the  $k$ -point or uniform crossovers.

Unfortunately, as we have discussed, these simple crossover operators are ineffective for spatial applications because they are spatially unaware. Indeed, this was the impetus for deriving new EA operators for spatial optimization where we designed the spatially cognizant PRCRX operator to produce both larger movements and enable a more diversified search. Our empirical evaluation showed that PRCRX offered significant improvement in both the effectiveness and the efficiency of the optimization search process (Liu and Cho, 2020), making it an auspicious prospect for an MCMC transition. Adaptation of PRCRX into an MCMC context, however, is not as simply realized as it is for the common and basic binary EA crossover operators.

<sup>1</sup>Fifield et al. (2019) bypass the need for computational advancements by proposing an approximation for the transition probability,  $p! \left(\frac{1}{u_x}\right)^p$ . However, their approximation is based on intuition and was not theoretically derived. They acknowledge that “it is difficult to develop a rigorous theoretical justification for the proposed approximation.” In addition, while they provide an empirical example, the closeness of this approximation to the true value is unknown in general and has not been rigorously tested or evaluated.

### 4.3 The Spatial Path Relinking Crossover

We adapt PRCRX, the spatial path relinking crossover operator that we developed as part of an optimization heuristic, to an MCMC algorithm through the Multiple-Try Model framework. Here, the purpose of the optimization crossover operator is to create a Markov transition *proposal set*. One proposal state from this set is chosen probabilistically and is accepted or rejected according to a generalized Metropolis-Hastings ratio.

We begin with a set of  $q$  parallel chains,  $\mathbf{X}_1, \mathbf{X}_2, \dots, \mathbf{X}_q$ , that are randomly generated. Their state at time  $t$  is  $\mathbf{x}_1^{(t)}, \mathbf{x}_2^{(t)}, \dots, \mathbf{x}_q^{(t)}$ , respectively. For the spatial path relinking crossover, we need a current state and a target state. If, at time  $t$ , for chain  $\mathbf{X}_i$ , we want to invoke a spatial path relinking crossover transition, then state  $\mathbf{x}_i^{(t)}$  becomes the current state. We randomly select another chain,  $\mathbf{X}_j, j \neq i$  from the set or population of all other Markov chains. The current state of that randomly chosen chain,  $\mathbf{x}_j^{(t)}$ , becomes the target state.<sup>2</sup> Roberts and Gilks (1994) established that essentially any way of choosing the target state,  $\mathbf{x}_j^{(t)}$ , is appropriate provided that  $\mathbf{x}_i^{(t)}$  and  $\mathbf{x}_j^{(t)}$  are independent.

The spatial path relinking crossover, PRCRX, begins at state  $\mathbf{x}_i^{(t)}$  and moves in the direction of state  $\mathbf{x}_j^{(t)}$ . Each step in the crossover heuristic involves the swap of some set of contiguous units from their zone in the current state to their zone in the target state. Figure 4 illustrates this process. The current state is shown in subfigure (a). The target state is shown in subfigure (b). Each of the outlined regions in subfigure (c) has a unique source/target zone label, indicating its zone assignment in the source state and its zone assignment in the target state. Since there are 4 zones, there are  $4 * 4 = 16$  possible unique current/target zone labels, though all of these zone labels will not necessarily be in an overlap. In the illustration, only 13 of the 16 possible groupings appear.

The path relinking begins with a set of  $k$  seed groups, where  $k$  is the number of zones in the partitioning problem. These seed groups can be chosen in any way as long as the resulting groups each have unique target zones. Subfigure (d) shows one way in which to choose these seed groups, i.e., by picking those groups where the current and target zone labels are the same.

Figure 4 shows one possible path that traverses the entire distance from the source state to the target state. Note that full traversal of the path from the current state to the target state is not necessary since the purpose is simply to explore the feasible intermediate states in the neighborhood space, not necessarily to complete the path. Subfigure (f) shows one intermediate state along one path that results from the re-assignment of the region labeled  $\Delta_1$ . Many intermediate/proposal states exist along the various possible paths in the spatial neighborhood space.

Let  $C$  be the total number of sets of contiguous units that need to be moved or re-assigned to complete the path. A proposal state is the result of the swap of some number,  $c$ , of these components,  $1 < c < C$ . The distance between states  $\mathbf{x}_i^{(t)}$  and  $\mathbf{x}_j^{(t)}$  is defined as  $d = \sum_{z=1}^C |G_z|$ , where  $z$

<sup>2</sup>The MTM framework requires  $T(\mathbf{x}, \mathbf{y}) > 0$  if and only if  $T(\mathbf{y}, \mathbf{x}) > 0$ . That is, the transition to  $\mathbf{y}$  from  $\mathbf{x}$  is possible if and only if this transition is reversible with non-zero probability. To ensure that  $\mathbf{x}$  could be chosen as the anchor solution, whenever a path relinking transition is accepted, we enlarge the target pool by one by inserting the current solution,  $\mathbf{x}_i^{(t)}$ , into the target pool. Since we just traversed a path that connects  $\mathbf{x}$  to  $\mathbf{y}$ , we know such a path exists. Hence, if  $\mathbf{y}$  becomes the current state, to satisfy the reversibility requirement, it only has to be possible that  $\mathbf{x}_i^{(t)}$  could be chosen as the target solution.

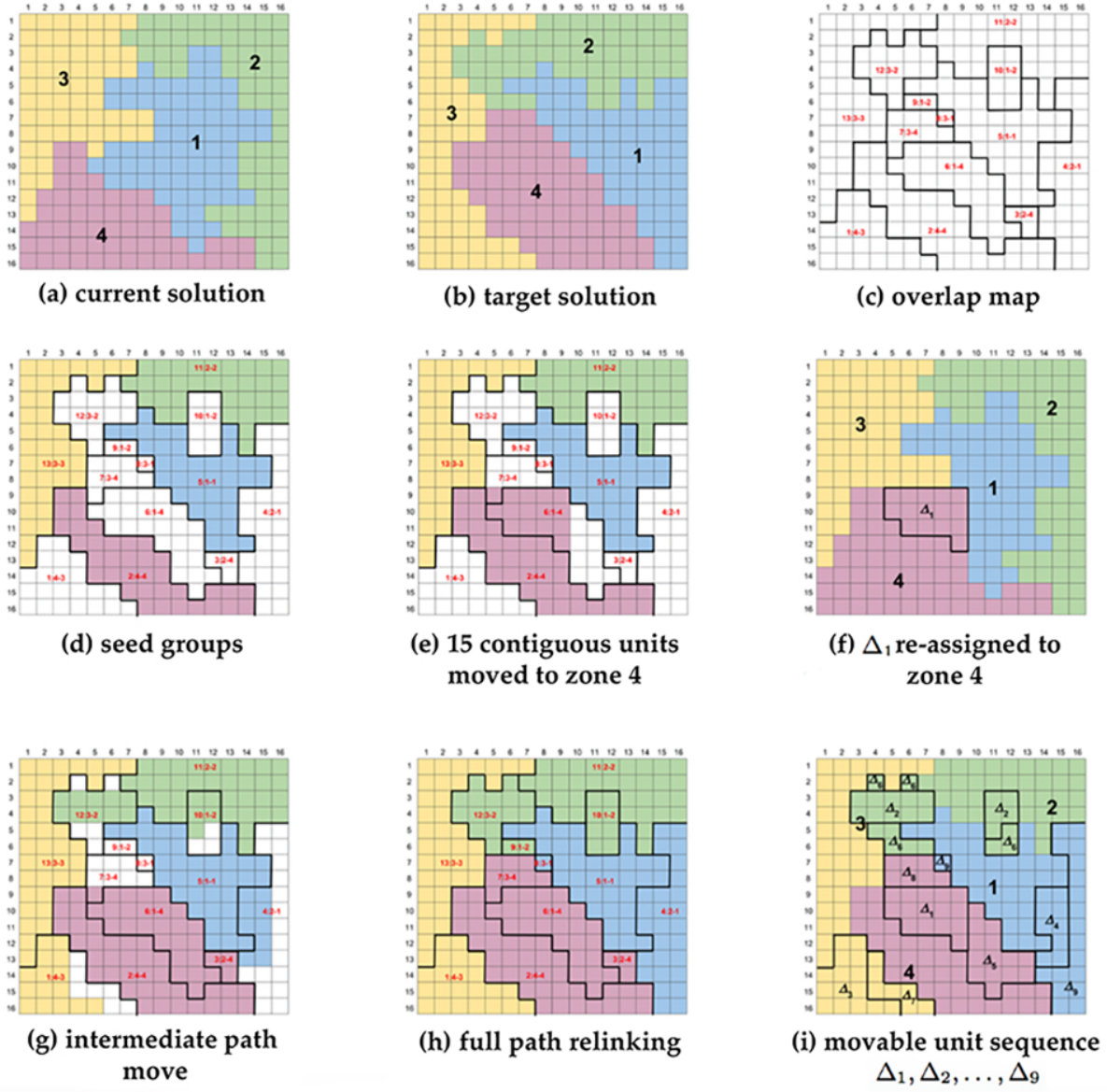


Figure 4: Illustration of the Crossover Operator (PRCRX)

is a zone identifier,  $G_z$  is a set of contiguous units,  $C$  is the number of sets,  $G_z$ , in the source zone that can potentially be moved to the target zone, and  $|G_z|$  is the cardinality of the set of contiguous units in the group  $G_z$ . At most,  $d$  units, contained within  $C$  connected components need to be moved to complete the entire path from the current state to the target state.

The direction of the movement from the current state is determined by the target state. The magnitude of the movement in this direction is chosen randomly by sampling  $d_m \sim \text{Unif}[\{|G_z|_{\forall z}\}]$ . To identify a set of  $m$  proposal states,  $\mathbf{y}_1, \mathbf{y}_2, \dots, \mathbf{y}_m$ , at various distances,  $d_m$ , along the path in the spatial neighborhood space of state  $\mathbf{x}_i^{(t)}$  and state  $\mathbf{x}_j^{(t)}$ , we draw  $m$  samples.

Once we have our proposal set,  $\mathbf{Y} = \{\mathbf{y}_1, \mathbf{y}_2, \dots, \mathbf{y}_m\}$ , we choose a state,  $\mathbf{y}$ , from this set with probability proportional to  $\xi(\mathbf{x}, \mathbf{y}) = \pi(\mathbf{x}) T(\mathbf{x}, \mathbf{y}) \lambda(\mathbf{x}, \mathbf{y})$ , where  $\lambda(\mathbf{x}, \mathbf{y})$  is a non-negative symmetric function and  $T(\mathbf{x}, \mathbf{y})$  is the proposal transition function defined by the path relinking operator. Note that  $T(\mathbf{x}, \mathbf{y})$  does not need to be symmetric. In addition, the only requirement for  $\lambda(\mathbf{x}, \mathbf{y})$  is that  $\lambda(\mathbf{x}, \mathbf{y}) > 0$  whenever  $T(\mathbf{x}, \mathbf{y}) > 0$ . How to identify an optimal  $\lambda(\mathbf{x}, \mathbf{y})$  for a particular application is an open question. However, Liu, Liang and Wong (2000), in their set of numerical experiments, found that the performance of an MTM sampler was insensitive to the choice of  $\lambda(\mathbf{x}, \mathbf{y})$  and that the simplest choice is  $\lambda(\mathbf{x}, \mathbf{y}) \equiv 1$ . This is the choice we utilize.

If  $c$  connected components is the number of connected components that have been moved from the current state  $\mathbf{x}$  to the target state,  $\mathbf{y}$ , then we can see that  $T(\mathbf{x}, \mathbf{y}) = C(C-1) \dots (C-(c-1))$  and then  $\xi(\mathbf{x}, \mathbf{y}) = T(\mathbf{x}, \mathbf{y}) \exp\{H(\mathbf{y})\}$ .

Once the state  $\mathbf{y}$  is chosen, we generate a second set,  $\{\mathbf{x}^*\} = \{\mathbf{x}_1^*, \mathbf{x}_2^*, \dots, \mathbf{x}_{m-1}^*\}$ , from  $T(\mathbf{y}, \cdot)$ , which is a transition that is also defined by the spatial path relinking model, but  $\mathbf{y}$  is now the current state,  $\mathbf{x}_i^{(t)}$  is the target state, and  $\{\mathbf{x}^*\}$  is a set of intermediate states that lie in the neighborhood space between  $\mathbf{y}$  and  $\mathbf{x}_i^{(t)}$ . We then accept  $\mathbf{y}$  as the next Markov chain state with probability defined by the generalized Metropolis-Hastings ratio,

$$r_{\text{PRCRX}} = \min \left\{ 1, \frac{\xi(\mathbf{y}, \mathbf{x}) + \sum_{j=1}^{m-1} \xi(\mathbf{y}_j, \mathbf{x})}{\xi(\mathbf{x}, \mathbf{y}) + \sum_{j=1}^{m-1} \xi(\mathbf{x}_j^*, \mathbf{y})} \right\}, \quad (15)$$

and let  $\mathbf{x}_i^{(t+1)} = \mathbf{x}_i^{(t)}$  with the remaining probability.

This process allows us to update one Markov chain,  $\mathbf{X}_i$ , with information from another Markov chain,  $\mathbf{X}_j$ , that is randomly chosen to be the target chain. The next step,  $\mathbf{x}_i^{(t+1)}$ , for the current Markov chain,  $\mathbf{X}_i$ , is updated with an MTM transition along the direction defined by the path between  $\mathbf{x}_i^{(t)}$  and  $\mathbf{x}_j^{(t)}$ .

#### 4.4 Evolutionary Markov Chain Monte Carlo Algorithm (EMCMC)

Our Evolutionary Markov Chain Monte Carlo (EMCMC) algorithm combines the advantages of evolutionary algorithms as optimization heuristics for state space traversal and the theoretical convergence properties of Markov Chain Monte Carlo algorithms for sampling from unknown distributions. We encompass these two algorithms within the framework of a Multiple-Try Metropolis Markov Chain model that incorporates a generalized Metropolis-Hasting ratio. The general framework is as follows.



1. Initialize  $q$  parallel chains,  $\mathbf{X}_1, \mathbf{X}_2, \dots, \mathbf{X}_q$  at separate randomly generated feasible solutions,  $\mathbf{x}_1^{(0)}, \mathbf{x}_2^{(0)}, \dots, \mathbf{x}_q^{(0)}$ .
2. For each iteration of the algorithm,  $t = 0, 1, \dots, T$ , the current state of each chain,  $\mathbf{x}_i^{(t)}$ , is updated to  $\mathbf{x}_i^{(t+1)}$ . The state at iteration  $t + 1$  is determined with either a mutation transition, with probability  $p_m$ , or a crossover transition, with probability  $p_c = 1 - p_m$ . The values of  $p_m$  and  $p_c$  may be the same or different across the  $n$  chains.
3. If the next step is determined with a mutation transition, generate a proposal transition via the ECMUT operator, and accept or reject that proposal with MH ratio,

$$r_{MUT} = \frac{M_x}{M_y} \exp\{-[H(\mathbf{y}) - H(\mathbf{x})]\}.$$

4. If the next step is a proposal from the PRCRX spatial path relinking crossover operator, accept the proposal with the generalized Metropolis ratio,

$$r_{PRCRX} = \min \left\{ 1, \frac{\xi(\mathbf{y}, \mathbf{x}) + \sum_{j=1}^{m-1} \xi(\mathbf{y}_j, \mathbf{x})}{\xi(\mathbf{x}, \mathbf{y}) + \sum_{j=1}^{m-1} \xi(\mathbf{x}_j^*, \mathbf{y})} \right\}.$$

By adapting the ECMUT mutation operator and the spatial PRCRX crossover operators into the MCMC framework as described in Sections 4.1–4.3, we arrive at a new MCMC algorithm, which we term an Evolutionary Markov Chain Monte Carlo algorithm (EMCMC), for sampling constrained spatial partitions. EMCMC utilizes optimization heuristics to guide the movement of Markov chains. This enables large movements in the state space while supplying a way for these large movements to identify states that are not unlikely to be associated with a reasonably large Metropolis-Hastings ratio. The Multiple-Try Method provides a generalized Metropolis-Hastings ratio that enables the integration of optimization methods with MCMC algorithms that is able to sampling spatial partition with constraints from spatial state spaces.

## 5 Empirical Example

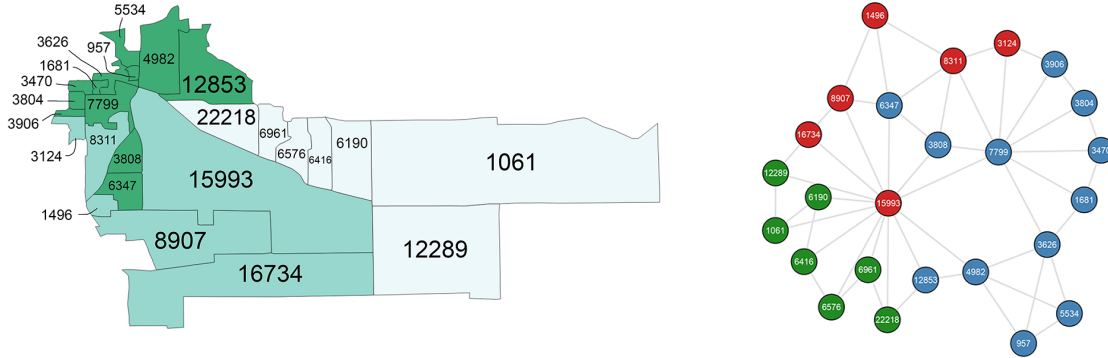


Figure 5: Spatial Partitioning Example. A representation with spatial geographic units is shown on the left. A graph representation is shown on the right.

We demonstrate the properties and effectiveness of EMCMC with an empirical application. In this application, there are 25 spatial units that we seek to partition into 3 spatially contiguous and separate zones. The plot on the left in Figure 5 shows these units and their spatial configuration as a collection of spatial geographic units. This representation is not particularly conducive to computational structures, and so we transform these units into a graph theory format. The corresponding graph theory representation is shown on the right in Figure 5. The edges in the graph indicate spatial adjacency. Each node is able to preserve the attributes of the geographic unit via node weights/attributes. The unit weights are shown by the number in each of the nodes.

In this example, a feasible solution is defined as an exhaustive and mutually exclusive partition of the 25 nodes into 3 disjoint contiguous subgraphs such that the total weight in each subgraph is within 10% of the total weight in each of the other subgraphs. The coloring in the map and the graph displays one feasible partition of the units into 3 zones/subgraphs that satisfy the contiguity and weight balancing requirement. The total weight of the red subgraph in the graph is 54,565. The total weight of the green subgraph is 61,711. The total weight of the blue subgraph is 58,767. If we measure the weight balance as  $\max_i |w_i - \mu|/\mu$ , where  $\mu = \sum_i w_i/k$ , and  $k$  is the number of zones, then this partition has a weight balance score of 0.058, which is below our threshold value of 0.10. We seek to produce a uniform sample of the set of all such feasible partitions.

With no constraints (i.e., no contiguity requirement and no weight balancing requirement), there are  $S(25, 3) = 141,197,991,025$  ways to partition these spatial units into 3 zones, where  $S(n, k)$  is a Sterling number of the second kind. When a contiguity requirement is imposed, the number of feasible partitions reduces to 117,688 possible solutions. When the weight balancing requirement is added, only 927 of the possible partitions remain feasible partitions. Evidently, the constraints significantly reduce the feasible portion of the overall state space.

We employed our EMCMC algorithm with 16 parallel chains. In 5 seconds of time, each chain visited approximately 7,000 feasible states or partitions where feasible is defined as satisfying the contiguity and the weight balancing requirements. Let  $X$  represent a feasible state. Since these states are spatial partitions, the state space does not have a convenient structure that is simple

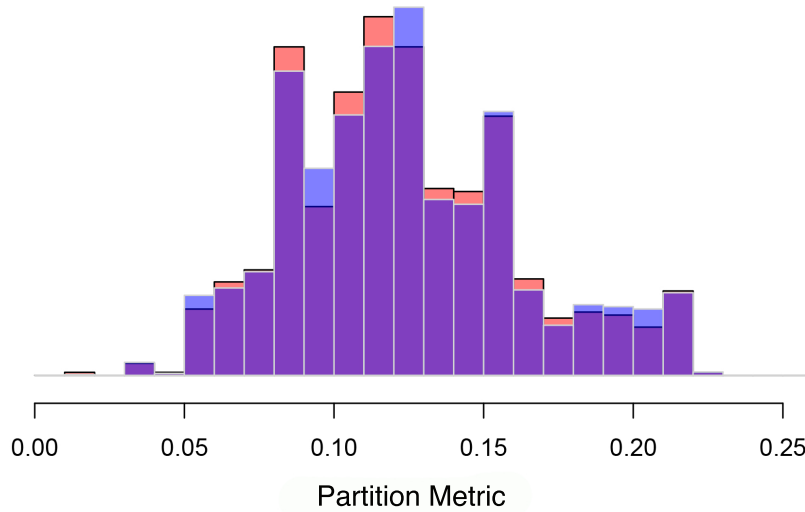


Figure 6: Spatial Partitioning Application Example. The true underlying distribution of the partition metric,  $f(X)$ , is shown with a red histogram. Overlaid on that red histogram is a blue histogram that shows the metric for the states visited by our Markov chains. In purple is the overlap of these two distributions.

either to order or to represent in  $\mathbb{R}$ . To alleviate this problem, let  $f : X \rightarrow \mathbb{R}$  be a function that takes a partition,  $X$ , and maps it to a metric in  $\mathbb{R}$ . This function may be an arbitrary function. The partition metric we use in our empirical example is,

$$f(X) = \frac{1}{2} \sum_{i=1}^k \frac{w_i}{\sum_{i=1}^k w_i} \frac{|r_i - R|}{R(1 - R)}, \quad (16)$$

where  $i = 1, \dots, k$  is a zone index,  $w_i$  is the aggregated weight in zone  $i$ ,  $r_i$  is the proportion of weight in zone  $i$  with a particular characteristic,  $r$ , and  $R$  is the proportion of that characteristic,  $r$ , across all zones. The resulting distribution of this partition metric,  $f(X)$ , among the visited states is shown in Figure 6. The true underlying distribution of the partition metric is shown with a red histogram. Overlaid on that red histogram is a blue histogram that shows the metric for the states visited by our Markov chains. In purple is the overlap of these two distributions. As we can see, the overlap of the states visited by the Markov chains and the true underlying distribution, while not exact, is fairly close. The histograms and their overlap provide evidence of the ability of our EMCMC algorithm to uniformly sample the underlying spatial state space.

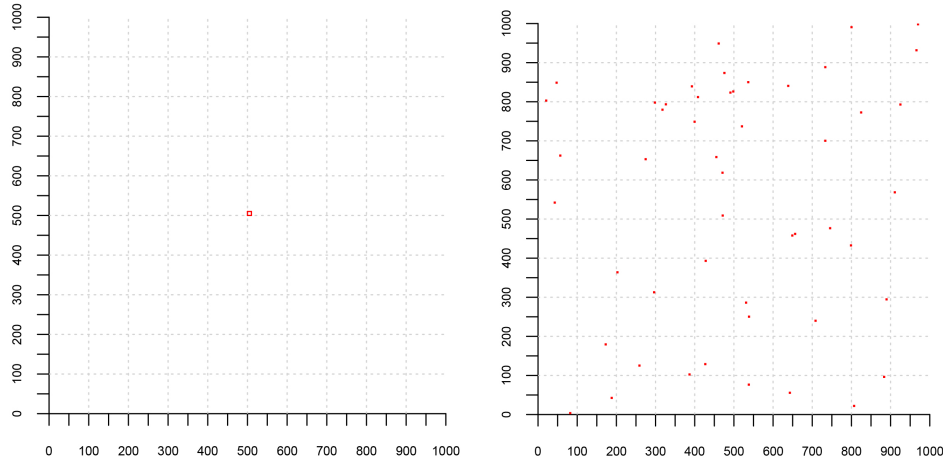


Figure 7: Visualizing the state space and the portion of the state space that contains feasible solutions. The set of feasible solutions is greatly reduced from the full set of combinatorial set partitions. The individual feasible solutions are scattered about the solution space in an unstructured and unknown manner.

## 6 The Challenges with Scaling to Larger Applications

While EMCMC was able to successfully sample the feasible spatial partitions in this spatial state space, this particular spatial partitioning application, while not trivial, is still small in size and does not reach the level of complexity that accompanies both larger problem sizes and/or additional constraints. Hence, while this spatial state space provides some proof of concept, additional hurdles must be overcome in order to ensure successful navigation for more complex applications. While our small example does not, itself, produce a sufficiently challenging application, it has two important roles. First, it is small enough that we can enumerate all of the spatial partitions and thus allows us to test the ability of our algorithm to produce a uniform sample from the true underlying distribution. Second, it is large enough to allow us to explore the structure and root of the obstacles that manifest in larger and more complex applications.

### 6.1 Solution Sparsity

One issue is solution sparsity. In our small problem, the simple unconstrained combinatorial construction of sets has more than  $10^{11}$  possible solutions. When the spatial contiguity constraint is imposed, the number of feasible partitions is reduced many orders of magnitude to  $10^5$ . That is, fewer than 0.0001% of the set partitions are spatially contiguous. Though it is obvious that considerations of spatially defined locality and adjacency have a direct and explicit effect on solution feasibility, this example highlights that even in a small sized application, the effect is dramatic.

Figure 7 helps us visualize the precipitous decline in the number of feasible solutions from the number of unconstrained combinatorial set partitions. In the figure on the left, if the plot region represents the full set of combinatorial set partitions, then the red square in the middle is *100 times*

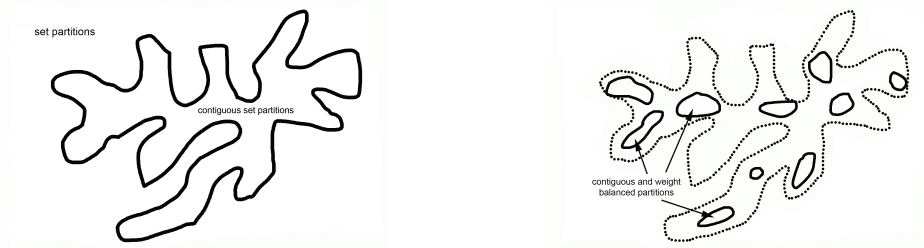


Figure 8: The figure on the left illustrates a fully connected subspace that is comprised of all solutions that satisfy the contiguity constraint. The figure on the right illustrates the patchy space that ensues if any constraint in addition to contiguity is used to define a feasible solution.

larger than the set of contiguous partitions. Pointedly, the feasible state space is *much* smaller than the entire decision space.

## 6.2 Disconnected Solution Space

While the red square helps us visualize the size of the feasible space, note that the feasible solutions are not concentrated in the central part or in *any* part of the entire solution space. Instead, the feasible solutions are scattered throughout the decision space in an unstructured and unknown manner, as illustrated in the plot on the right in Figure 7. While the size of the dots is now too large (collectively, they should be 100 times smaller than the red square in the plot on the left), they are correctly shown as scattered throughout the space. For any reasonably sized spatial partitioning problem, then, an intelligent spatially guided search is essential since simply random movement in the decision space almost surely identifies an infeasible solution, which results in enormous wasted computational effort (Liu and Cho, 2020).

Importantly, note the critical implications that arise from the choice of the graph theoretic representation. Computationally, the graph theoretic framework is advantageous because it permits a simple way to incorporate spatial adjacency with convenient discrete structures and provides an organizational framework for state space traversal. It also facilitates a way to define a fully connected state space such that beginning at any contiguous state, one can reach any other contiguous solution via a sequence of deletions/creations of single edges between nodes. Unsurprisingly, accounting for contiguity in this graph traversal is relatively simple since the basis of the graph structure is spatial contiguity. However, perhaps also unsurprisingly, then, graph traversal accounting for other constraints is not so easily facilitated and requires dedicated effort and ingenuity.

To be sure, any graph theoretic framework compels a specific notion of solution adjacency and proximity. In particular, the number of edges that must be changed to convert one solution to another defines the distance between those two solutions in the state space. In our graph representation, the distance from one contiguous solution to another contiguous solution is 1; and the set of all contiguous solutions forms a connected set. When feasibility includes another constraint, this additionally constrained set of feasible solutions, using this graph traversal mechanism, almost surely now comprises a disconnected set.

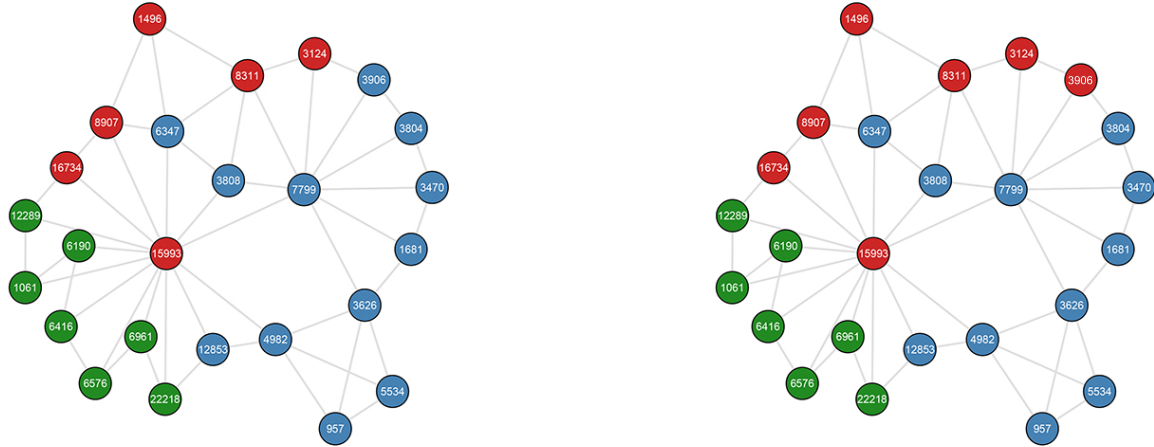


Figure 9: Spatially Isolated Partitions. With a Markov transition that involves only movement on zone boundaries, these two feasible partitions are isolated from all other feasible partitions.

A connected space can be visualized with the amoeba shape shown in Figure 8. The main feature of the “shape” of the contiguous solutions is that it comprises a connected subspace such that any contiguous partition can be reached from any other contiguous partition with transitions that traverse only other contiguous partitions. That is, movement is completely confined within the contiguous set, and movement into infeasible space is not necessary. However, the imposition of any other constraint, say, weight balancing, induces a “patchy” decision space that is not fully connected by similar traversal. We can visualize this as the figure on the right in Figure 8. How to traverse from one contiguous solution that satisfies the weight balancing criterion to another contiguous solution that also satisfies the weight balancing criteria is non-trivially more difficult, featuring not only greater sparsity, but disconnected solution regions. For our small example, Figure 9 shows two feasible partitions that are proximate and reachable from the other, but isolated from *all* other feasible partitions if traversal involves only unit swaps on subgraph borders.

### 6.3 Search Strategies

As we have already noted, for the task of sampling solutions satisfying only the contiguity constraint, a Markov transition like ECMUT-1, as well as variants that have been proposed by others (Bangia et al., 2017), is sufficient. While the Markov chain produced by this transition proposal is irreducible on the fully connected state space, it is not irreducible when additional constraints restrict the feasible solution space and induce a disconnected state space. A reducible Markov chain will not produce a sample of the underlying space.

This issue can be resolved by 1) allowing movement into infeasible space in the search for other feasible regions, 2) formulating a set of parallel or serial chains that uniformly sample among and in the disconnected regions, or 3) specifying a different transition proposal that does produce an irreducible Markov chain. The first option is theoretically viable, but plainly produces massive computational waste. In our small example, the wasted effort is not strictly limiting given the small problem size. However, for a larger and more realistic application, this approach is not

practical without enlisting greater computational capacity. The second option avoids the wasted computational effort spent wading through infeasible regions, but then introduces a new problem to solve, that of identifying a random sample of initial states. For our small spatial partitioning application, and for applications generally where the state space is not continuous, parallel Markov chains can alleviate some of the potential issues if we are able to generate random initial states in different disconnected regions. For our small empirical application, generating these initial random states was relatively easy, but for larger and more complex applications, devising a method for identifying random initial states for a set of parallel chains is non-trivial. The third option requires ingenuity in devising the transition proposal for the Markov chain. The transition proposal must be able to make large movements that transcend the discontinuities that vex simpler and smaller transition proposals.<sup>3</sup>

Certainly the advantages of employing these separate options can be made more effective by combining the various strategies. Movement need not completely avoid infeasible solutions; parallelism can be implemented from a variety of different serial scenarios; and larger Markov transitions can be integrated along with parallel chains that sometimes explore infeasible space. Indeed, a confluence of these strategies is likely to be more effective than any one on its own. This is the approach that we employ in our EMCMC algorithm, where all of these strategies have been incorporated.

Finally, computational scalability transcends the choice of search strategy. While convergence rates are certainly affected by the efficiency of the transition proposal, for large applications, one must also pursue computational strategies to further improve efficiency. This brings us to our last challenge, where even with a significantly more efficient and irreducible Markov chain, the issue of *scalability* remains.

## 6.4 Computational Scalability with Massively Parallel Architecture

The nature of the EMCMC algorithm is already parallelized, with a parallel structure that is straightforward to scale, so scalability is already an integral part of our algorithm. In Figure 10, we see how our EMCMC algorithm scales when we enlist more processor cores. As we double the number of processor cores, EMCMC reaches an increasingly larger portion of the underlying state space. The figure on the right shows the number of unique solutions identified in 10 minutes

---

<sup>3</sup>To be sure, there may be other issues such as a multimodal state space replete with copious low and high energy states. Here, there is a significant literature with many and varied proposals. None of these can be regarded as a general fix. Rather, they must be tuned to the particular application. The strategies generally fall into one of two camps. The first is the set of methods that incorporate temperature as an auxiliary variable to facilitate sampling at a broad array of temperatures, both low and high. Included in this set is, for example, parallel tempering (Geyer, 1991), the equi-energy sampler (Kou, Zhou and Wong, 2006), and the Swendsen-Wang algorithm (Swendsen and Wang, 1986). The second is the set that incorporates information from past samples, which includes, for example, multicanonical sampling (Berg and Neuhaus, 1991), the Wang-Landau algorithm (Wang and Landau, 2001) and stochastic approximation Monte Carlo (Liang, Liu and Carroll, 2007). The choice depends on which strategy is most tightly coupled with the peculiarities of the specific state space. This literature addresses issues of efficiency in the Markov chain. That is, if one has an irreducible Markov chain that converges slowly, these strategies help to increase the efficiency of that chain and hasten convergence by producing a method that employs a mechanism for facilitating movement out of low energy states. Fifield et al. (2019) found that a parallel tempering approach was able to sample spatial partitions, but they failed to realize that the sample was enabled by the different chains that were initialized in different disconnected regions. That is, what makes this approach tenable is not parallel tempering per se, but the ability to initiate different Markov chains (whether in parallel or not) at different and random starting states.

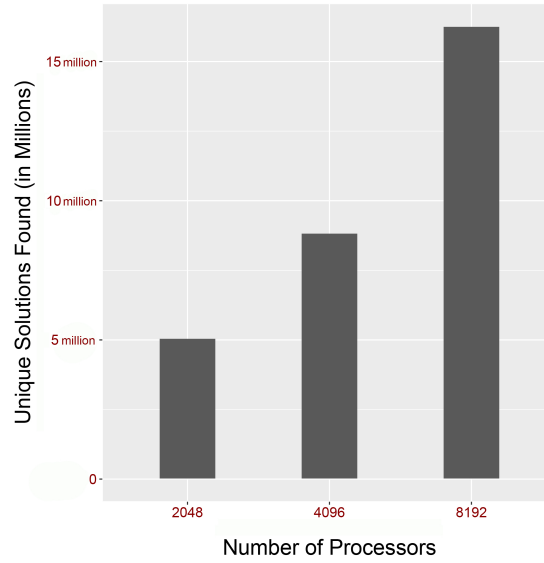


Figure 10: Scalability of EMCMC Algorithm. EMCMC is able to effectively scale with additional computational resources.

of computing time on the Blue Waters supercomputer. When 8,192 processors are utilized, we explore almost 17 million unique states, which is more than 3 times as many states as were explored with 2,048 processor cores. Importantly, with any number of processor cores, the EMCMC algorithm was able to parse the underlying state space to successfully produce a representative sample of the set of feasible solutions.

As the size of the state space grows larger, all of the challenges we have identified must be addressed simultaneously and in increasingly adept ways. Indeed, as the application size grows, the effectiveness and efficiency afforded by the spatial path relinking crossover transition becomes increasingly essential. The crossover transition provides both larger movement, leading to greater efficiency and effectiveness, as well as the ability to move between disconnected portions of the overall state space. Our directed crossover operator guides intelligent and efficient space traversal while parallel chains aid in diversity, reaching the different modes, and harnessing more computing power. In this small example, the power of PRCRX was not evident because the space is sufficiently small that it can be effectively sampled with the ECMUT operator and parallel chains that were initiated at different random start states. This strategy would not be effective with larger applications where our spatial path relinking crossover and our ability to harness massive computing power becomes essential.

## 7 Discussion

We have devised a massively parallel Evolutionary Markov Chain Monte Carlo (EMCMC) algorithm for sampling from astronomically large and complex spatial state spaces. The applicability and performance of our algorithm has been demonstrated for a spatial partitioning problem. We



have additionally scaled our algorithm to harness massive computational power on parallel computing architecture, which is necessary for problems of large scale. The performance gain of our algorithm is significant.

Within our EMCMC algorithm, we have introduced a transition rule for a Markov chain that utilizes an optimization heuristic to enable large movements. Our optimization heuristic identifies local optimality information via a directed search. We use this information to adapt and update the Markov chain in promising directions. These ideas stem from Mezei (1980) and Gelman and Rubin (1992), who suggested that efficiency in a Markov chain can be improved by initially exploring where modes occur and then adjusting the proposal function accordingly, as well as the work of Liu, Liang and Wong (2000) who proposed the MTM method where any anchor point that is independent of the current state can be used effectively in an MCMC sampler to direct future draws. In addition, our work builds upon our previous research in the optimization realm, which we utilize to form the basis for an adaptive deterministic procedure in our MCMC.

There remain a number of avenues for future exploration. For instance, the efficiency of the EMCMC sampler relies on a calibration between the proposal step size, the size of the proposal set,  $m$ , and the complexity of the landscape of the underlying distribution,  $\pi$ . As well, while our EA operators were effective, there are other and perhaps more efficient methods for landscape traversal in these spatial state spaces. Improvement in the optimization components would have obvious translation to gains in performance for the sampler. There is an unknown and untested relationship between the population size or the number of parallel chains and the rate of convergence of the sampler. A larger number of chains increases the diversification of the search, which is desirable, while fewer but longer chains have an impact on the convergence rate. There are a number of trade offs, some of which are application specific, while others have roots in the theoretical properties of the underlying model.

In addition, computational advances will improve the performance of the sampler. This includes innovations that increase the efficiency of the computational algorithms as well as novel ways to adapt the serial implementation of the algorithm to run on the massively parallel architecture that is available on supercomputers. This type of architecture will have an obvious relationship with the population size or the number of Markov chains that can be run in parallel. It has a more subtle relationship with how the search can be made more efficient, by perhaps, intelligently increasing the diversity and the intensity of the optimization heuristic in response to the variations in state space landscape (Cho and Liu, 2019). The large number of processors could then span across the solution space to increase diversity in the search while working collectively or intensively in regions where the search is particularly difficult.

## 8 Acknowledgements

This research is part of the Blue Waters sustained petascale computing project, which is supported by the National Science Foundation (awards OCI-0725070 and ACI-1238993) and the State of Illinois. Blue Waters is a joint effort of the University of Illinois at Urbana-Champaign and its National Center for Supercomputing Applications.

## References

- Bangia, Sachet, Christy Vaughn Graves, Gregory Herschlag, Han Sung Kang, Justin Luo, Jonathan C. Mattingly and Robert Ravier. 2017. "Redistricting: Drawing the Line." arXiv:1704.03360 stat.AP.
- Bélisle, Claude J.P., H. Edwin Romeijn and Robert L. Smith. 1993. "Hit-and-Run Algorithms for Generating Multivariate Distributions." *Mathematics of Operations Research* 18(2):255–266.
- Berg, Bernd A. and Thomas Neuhaus. 1991. "Multicanonical Algorithms for First Order Phase Transitions." *Physics Letters B* 267(2):249–253.
- Carlin, Bradley P. and Alan E. Gelfand. 1991. "An Iterative Monte Carlo Method for Nonconjugate Bayesian Analysis." *Statistics and Computing* 1(2):119–128.
- Cho, Wendy K. Tam and Yan Y. Liu. 2017. Massively Parallel Evolutionary Computation for Empowering Electoral Reform: Quantifying Gerrymandering via Multi-objective Optimization and Statistical Analysis. *SC17: The International Conference for High Performance Computing, Networking, Storage and Analysis*.
- Cho, Wendy K. Tam and Yan Y. Liu. 2019. Parallel Hybrid Metaheuristics with Distributed Intensification and Diversification for Large-scale Optimization in Big Data Statistical Analysis. In *Proceedings of the 2019 IEEE International Conference on Big Data*. Los Angeles, CA: .
- Duque, Juan C., Richard L. Church and Richard S. Middleton. 2011. "The p-Regions Problem." *Geographical Analysis* 43(1):104–126.
- Fifield, Benjamin, Michael Higgins, Kosuke Imai and Alexander Tarr. 2019. "A New Automated Redistricting Simulator Using Markov Chain Monte Carlo." Working Paper.
- Francis, Richard L. and John A. White. 1974. *Facility Layout and Location: An Analytical Approach*. Englewood Cliffs, NJ: Prentice Hall.
- Gelman, Andrew and Donald B. Rubin. 1992. "Inference from Iterative Simulation Using Multiple Sequences." *Statistical Science* 7:457–492.
- Geyer, Charles J. 1991. Markov Chain Monte Carlo Maximum Likelihood. In *Computing Science and Statistics: Proceedings of the 23rd Symposium on the Interface*, ed. E.M. Keramidas. Fairfax Station: Interface Foundations pp. 156–163.
- Gilks, W.R., G.O. Roberts and E.I. George. 1994. "Adaptive Direction Sampling." *The Statistician* 43(1):179–189.
- Glover, Fred. 1994. "Genetic Algorithms and Scatter Search: Unsuspected Potentials." *Statistics and Computing* 4(2):131–140.
- Glover, Fred, Manuel Laguna and Rafael Marti. 2000. "Fundamentals of Scatter Search and Path Relinking." *Control and Cybernetics* 29(3):653–684.

- Hastings, W. K. 1970. "Monte Carlo sampling methods using Markov chains and their applications." *Biometrika* 57(1):97–109.
- Hof, John G. and Michael Bevers. 1998. *Spatial Optimization for Managed Ecosystems*. New York: Columbia University Press.
- Kou, S.C., Qing Zhou and Wing Hung Wong. 2006. "Equi-energy Sampler with Applications in Statistical Inference and Statistical Mechanics." *The Annals of Statistics* 34(4):1581–1619.
- Laskey, Kathryn Blackmond and James M. Myers. 2003. "Population Markov Chain Monte Carlo." *Machine Learning* 50(1–2):175–196.
- Liang, Faming, Chuanhai Liu and Raymond J. Carroll. 2007. "Stochastic Approximation in Monte Carlo Computation." *Journal of the American Statistical Association* 102(477):305–320.
- Liang, Faming and Wing Hung Wong. 2000. "Evolutionary Monte Carlo Sampling: Applications to  $C_p$  Model Sampling and Change-point Problems." *Statistica Sinica* 10:317–342.
- Liang, Faming and Wing Hung Wong. 2001. "Real-Parameter Evolutionary Monte Carlo With Applications to Bayesian Mixture Models." *Journal of the American Statistical Society* 96(454):653–666.
- Liu, Jun S., Faming Liang and Wing Hung Wong. 2000. "The Use of Multiple-Try Method and Local Optimization in Metropolis Sampling." *Journal of the American Statistical Association* 95(449):121–134.
- Liu, Yan Y. and Wendy K. Tam Cho. 2020. "A Spatially Explicit Evolutionary Algorithm for the Spatial Partitioning Problem." *Applied Soft Computing Journal* .
- Liu, Yan Y., Wendy K. Tam Cho and Shaowen Wang. 2016. "PEAR: A Massively Parallel Evolutionary Computation Approach for Political Redistricting Optimization and Analysis." *Swarm and Evolutionary Computation* 30:78–92.
- Mattingly, Jonathan C. and Christy Vaughn. 2014. "Redistricting and the Will of the People." arXiv:1410.8796.
- Metropolis, Nicholas, Arianna W. Rosenbluth, Marshall N. Rosenbluth, Augusta H. Teller and Edward Teller. 1953. "Equation of State Calculations by Fast Computing Machines." *The Journal of Chemical Physics* 21(6):1087–1092.
- Mezei, Mihaly. 1980. "A Cavity-Based ( $T, V, \mu$ ) Monte Carlo Method for the Computer Simulation of Fluids." *Molecular Physics* 40:901–906.
- O’Kelly, Morton E and Harvey J. Miller. 1994. "The Hub Network Design Problem: A Review and Synthesis." *Journal of Transportation Geography* 2(1):31–40.
- Ritter, Christian and Martin A. Tanner. 1992. "Facilitating the Gibbs Sampler: The Gibbs Stopper and the Griddy-Gibbs Sampler." *Journal of the American Statistical Association* 87(419):861–868.

- Roberts, G.O. and W.R. Gilks. 1994. "Convergence of Adaptive Direction Sampling." *Journal of Multivariate Analysis* 49(2):287–298.
- Shirabe, Takeshi. 2009. "Districting Modeling with Exact Contiguity Constraints." *Environment and Planning B: Planning and Design* 36(6):1053–1066.
- Swendsen, Robert H. and Jian-Sheng Wang. 1986. "Nonuniversal Critical Dynamics in Monte Carlo Simulation." *Physical Review Letters* 58:86–88.
- Wang, Fugao and D.P. Landau. 2001. "Efficient, Multiple-Range Random-Walk Algorithm to Calculate the Density of States." *Physical Review Letters* 86(10):2050–2053.